iJRASET
International Journal For Research in Applied Science and Engineering Technology



INTERNATIONAL JOURNAL FOR RESEARCH

IN APPLIED SCIENCE & ENGINEERING TECHNOLOGY

Volume: 14 **Issue:** III **Month of publication:** March 2026

DOI: https://doi.org/10.22214/ijraset.2026.78425

www.ijraset.com

Call: 08813907089 | E-mail ID: ijraset@gmail.com

International Journal for Research in Applied Science & Engineering Technology (IJRASET)
ISSN: 2321-9653; IC Value: 45.98; SJ Impact Factor: 7.538
Volume 14 Issue III Mar 2026- Available at www.ijraset.com

Modelling and Simulation of an Off-Grid Photovoltaic System using Hybrid Energy Storage System for Electrification in Nigeria

T. C. Atasie[1], L. O. Uzoechi[2], S. O. Okozi[3]
[1, 2, 3]*Department Electrical and Electronics Engineering, Federal University of Technology, Owerri, Nigeria*

Abstract: ***In this work, the objectives of this research is to simulate the combination of a photovoltaic system with multiple energy system comprising of a battery and a supercapacitor. The results from the modelling of the photovoltaic system was compared with the current, voltage and power output of an LG datasheet. From the results obtained it was observed that when the area of the photovoltaic panel was reduced slightly by 0.01, the output current decreased by 0.001 but an increase in the area did not result in any significant change on the output current or voltage .This shows that the area of the photovoltaic panel does not affect the output current, voltage and power. During discharging mode (battery only), using a controlled current source which was connected to a load of 12.5A, State of Charge and current at 50% and 100AH respectively for 3,600s, we obtain*** I_{out} ***equals to 12.5A, SOC equals to 50% with*** V_{out} ***equals to 13.78V. Discharging occurs, although slowly. During charging mode (battery only), using a controlled current source which was connected to the load, at same voltage.We obtained SOC equals to 50.0007%,*** V_{out} ***equals to 13.81V, I equals to 10.0A. Charging occurs, also slowly. During discharging mode (battery and supercapacitor connected to the off-grid Photovoltaic panel to an AC load), at an initial SOC value equals to 50%, we obtain SOC equals to 49.95,*** I_{out} ***equals to 35A and*** V_{out} ***equals to 13.75. During charging mode (battery and supercapacitor connected to the off-grid Photovoltaic panel to an AC load), we obtain SOC equals to 50.31%,*** I_{out} ***equals to 220A,*** V_{out} ***equals to 14.07V. The output current and voltage of the off-grid photovoltaic system rose faster when connected to the supercapacitor.***
Keywords: Off-grid, Photovoltaic, Analytical modelling, Hybrid Energy Storage Systems (HESS), MatLab/Simulink.

I. BACKGROUND OF THE STUDY

One of the key design challenges for power systems operating primarily from renewable energy sources is that the generated power profile is unlikely to match the load requirement. For this reason, much attention is focused on development of novel energy storage systems for future renewable power applications. Recent technological advances have made the employment of high power density (>4kW/kg) and low energy density storage (<10Wh/kg) devices such as supercapacitors, advanced flywheel systems and superconducting-magnetic energy-storage system more technologically feasible (X. Qing, et al). Their combined use with more traditional energy storage systems such as electro-chemical batteries (which are more suited to longer-term storage, lower power/higher energy density applications) permits the key benefits of each to be employed.

The Photovoltaic systems can be mainly classified into different types of approaches, such as Standalone Photovoltaic (SAPV) systems, grid connected and hybrid arrangements. SAPV and hybrid systems are categorized into the form of distributed and centralized systems. In the distributed system, the system supplies the load demand individually. In the centralized system, the energy sources are located in the center of the loads, and the energy can supply to the customers considering the diversity of the load demand. A centralized system is cost-effective, and it has a smaller size as compared to the distributed system. The utilization of SAPV systems may drive to a shift of technology in terms of “living in off-grid” or “leaving the grid”. Besides, the transformed customers from the utility-grid can dissolve the worries of rising electricity bill. The SAPV system is an attractive and effective source of electricity in both the remote residential and commercial areas, (Ridha, H. M., & Gomes, C., 2020).

The growing global concern about environmental pollution and demand for energy encourages the use of solar energy. The basic element of a PV system is the solar cell, which consists of one or more p-n semiconductor junctions used for converting solar energy into electricity. The solar irradiance and the cell temperature influence the electricity generation of a solar cell. Parameters relating to module construction and interconnection and bypass diodes influence the performance. Circuit and mathematical models in the literature can represent the I-V and P-V characteristics of PV cells, modules or arrays. These models may represent non-linear PV characteristics at different levels of complexity, accuracy and processing speed, (Moreira, H. S., & Villalva, M. G., 2017).

©IJRASET: All Rights are Reserved

ISSN: 2321-9653; IC Value: 45.98; SJ Impact Factor: 7.538
Volume 14 Issue III Mar 2026- Available at www.ijraset.com

Global energy challenges and their impact on the environment have accelerated the adoption of renewable energy sources and development of smart and efficient micro-grid technologies. Low voltage micro-grid in particular has attracted increasing attentions from researchers. Micro-grid is a small-scaled autonomous power grid system that consists of multiple energy generations from renewable and non-renewables resources, energy storage systems (ESS) and power electronic converters. Micro-grid can be operated either in standalone mode or connected to the utility grid. A key advantage of micro-grid is that it allows power generation and supply to remote isolated community without the need for costly and inefficient long-distance high-voltage transmission and distribution infrastructures, (Jing, W., et al).

The possibility of converting solar radiation into electrical energy has made it suitable in many applications. Solar radiation can be converted into electricity using a photovoltaic (PV) system. Solar electricity may be used for power supply to remote villages and locations not connected to the national grid as well as to generate power for feeding into the national grid. Other common areas of application of solar electricity include low and medium power application such as water pumping, village electrification, rural clinic and school power supply, vaccine refrigeration, traffic lighting and lighting of road (Sambo, 2010). In Nigeria, most of the photovoltaic system employed to provide electricity service to rural communities for street lighting, water pumping, primary health centres, refrigerators and TV viewing centres are government-sponsored project (Agbonaye, O., & Odiase, F. O. , 2020).

II. METHODOLOGY

The research methods adopted in this work is also outlined as illustrated in Figure 1.

1) Firstly, mathematical equations that embody the essential principles governing the operations of a photovoltaic system was analytically modelled and simulated. A derived equation that takes the area of the photovoltaic module was also analytically modelled alongside the other equations and simulated using the Matlab/Simulink.
2) Secondly, a dynamic Hybrid Energy Storage System, which comprises of a Battery/Supercapacitor, was be modelled and simulated
3) Thirdly, the results obtained was compared with the LG module datasheet for validation.
4) Fourthly, the results obtained from off-grid battery-PV system and the off-grid battery-supercapacitor-PV system was compared to show the benefits of the off-grid battery-supercapacitor-PV system.

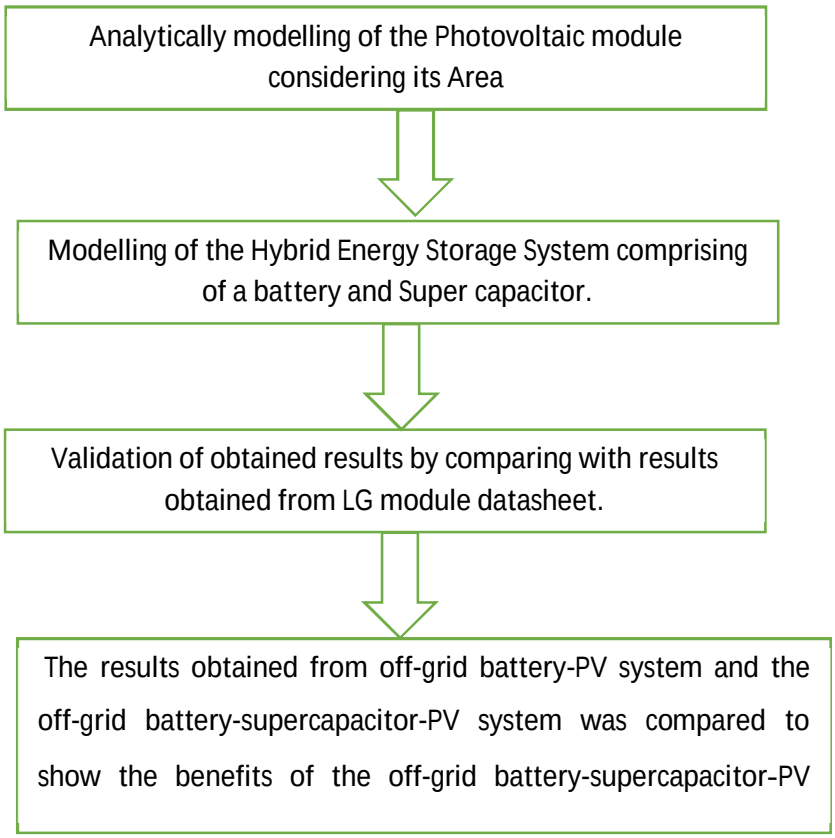


Fig. 2: Block Chart of the research method

©IJRASET: All Rights are Reserved

III. ANALYTICAL MODELLING OF THE PHOTOVOLTAIC SYSTEM

The analytical model is primarily quantitative or computational in nature and represents the system in terms of a set of mathematical equations that specify parametric relationships and their associated parametric values as a function of time, space and other system parameters. This is usually done by modelling certain underlying phenomenon to predict or assess how well the system performs or other characteristics.

The equation showing the relationship of the area of the Photovoltaic system as it affects the current is contained in the series current derivation.

The current rating of the diode in series is the same as the current rating of one of the diodes. In the reverse direction, both series diodes have the same reverse leakage current but different values for reverse voltage. **The series current**, Is, can be derived from the following:

The resistivity of a conductor, ρ such as a diode is the resistance per unit length and cross-sectional area at a certain temperature of a material which is represented in equation 1.

$$p = \frac{RA}{L} \quad (1)$$

Making R, the subject of the relation results in equation 2

$$R = \frac{pL}{A} \quad (2)$$

$$since\ V = IR \quad (3)$$

$$R = \frac{V}{I} \quad (4)$$

$$\frac{V}{I} = \frac{pL}{A} \quad (5)$$

$$IpL = VA \quad (6)$$

$$I = \frac{VA}{pL} \quad (7)$$

Where I is the series current which can also be written as I_s.

Fig. 3.2 is the representation of the equation in Eqn. 3 using Simulink blocks. These blocks are interconnected to produce the output which is then used to form a subsystem.

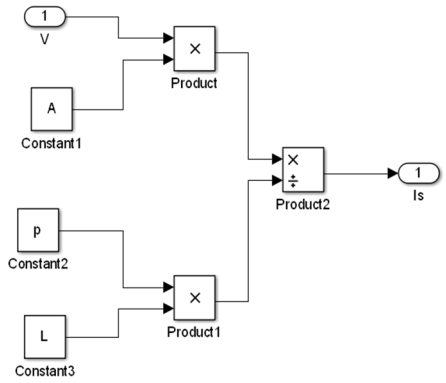


Fig 2.1: A model of Series current equation on Simulink

Fig. 2.2 is the subsystem of the equation in Fig. 2.1 which is combined to form a single system of an output and input.

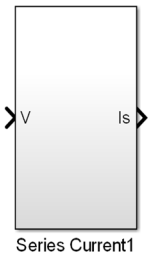


Fig 2.2: A subsystem of the Series Current on Simulink

The Photo Current, $\mathbf{I_{ph}}$, which is the electric current through a photosensitive device, such as a photodiode, because of exposure to radiant power can be calculated as follows:

$$I_{ph} = [I_{sc} + K_i(T - 298)]\left(\frac{G}{1000}\right) \quad 8$$

Where I_{sc} is the short circuit current, T is the operating temperature (K) and K_i is the short circuit current of cell at 25^0C. G is the solar irradiation absorbed. Fig. 3.4 is the representation of the equation in Eqn. 8 using Simulink blocks. These blocks are interconnected to produce the output which is then used to form a subsystem.

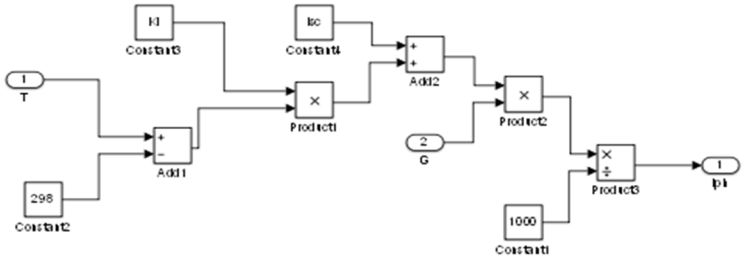


Fig 2.3: A model of photocurrent equation on Simulink

Fig. 2.4 is the subsystem of the equation in Fig. 2.3 which is combined to form a single system of an output and input.

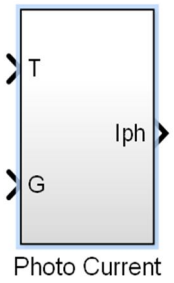


Fig 2.4: A subsystem of the photocurrent on Simulink

The saturation current, $\mathbf{I_0}$, which is the current in a semiconductor diode cause by the diffusion of minority of carriers from the neutral regions to the depletion region can be calculated as shown below:

$$I_0 = I_{rs}\left(\frac{T}{T_n}\right)3 \text{ x } \exp\left(\frac{qEgo\left(\frac{1}{T_n}-\frac{1}{T}\right)}{n*K}\right) \quad 9$$

Where Eg_0 is the Band Gap Energy of the semiconductor, T_n is the nominal temperature (K), K is the Boltzmann's constant (J/k), q is the electron charge and n is the ideality factor of the diode. Fig. 3.6 is the representation of the equation in Eqn. 9 using Simulink blocks. These blocks are interconnected to produce the output which is then used to form a subsystem.

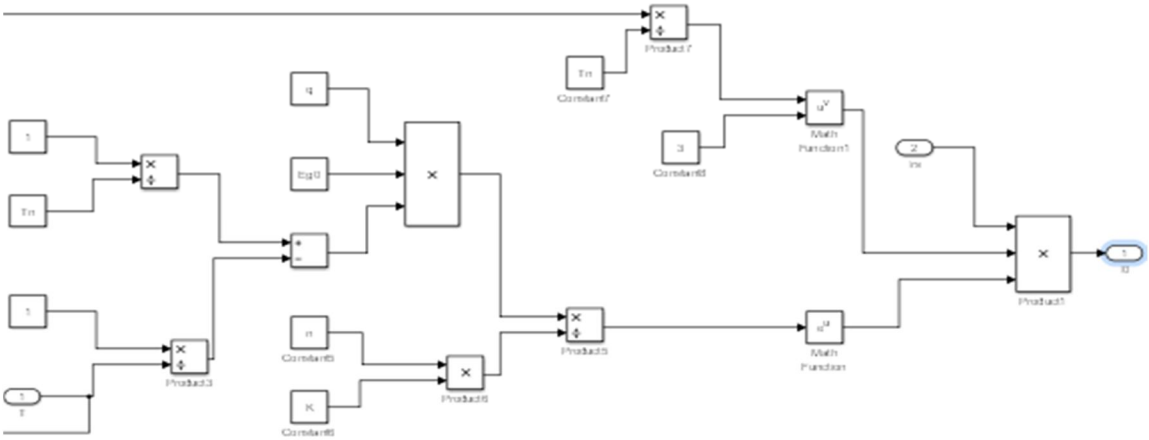


Fig 2.5: A model of Saturation current equation on Simulink

Fig. 2.6 is the subsystem of the equation in Fig. 2.5 which is combined to form a single system of an output and input.

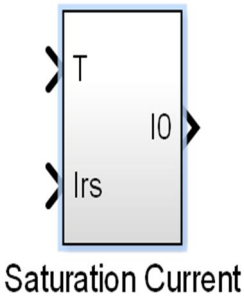


Fig 2.6: A subsystem of the Saturation current on Simulink

Reverse Saturation Current, I_{rs}, which is the part of the reverse current in a semiconductor diode caused by the diffusion of minority carriers from the neutral regions to the depletion region can also be calculated as follows:

$$I_{rs} = \frac{I_{sc}}{e\left(q*\frac{V_{oc}}{n}*N_s*K*T\right)} - 1 \qquad 10$$

Where V_{oc} is the open circuit voltage, N_s is the number of cells connected in series. Fig. 3.8 is the representation of the equation in Eqn. 10 using Simulink blocks. These blocks are interconnected to produce the output which is then used to form a subsystem.

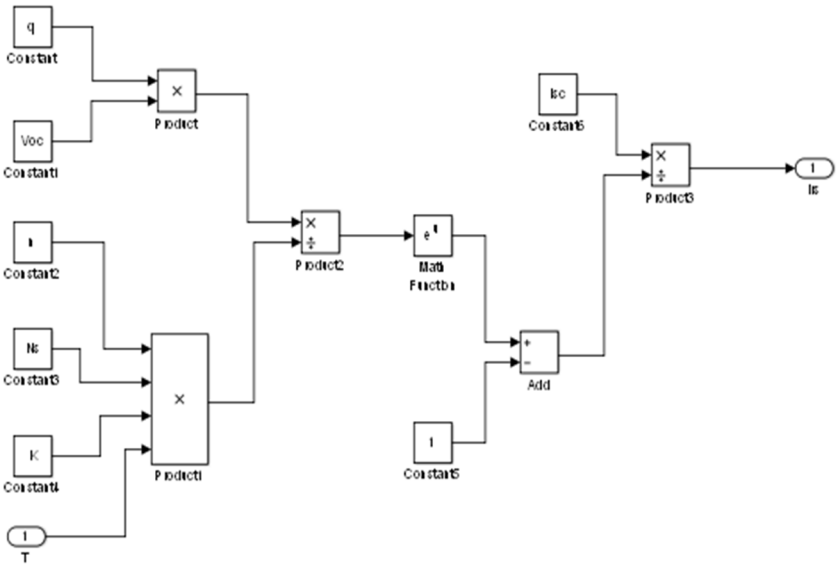


Fig 2.7: A model of Reverse Saturation current equation on Simulink

Fig. 2.8 is the subsystem of the equation in Fig. 2.7 which is combined to form a single system of an output and input.

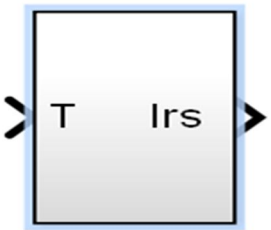


Fig 2.8: A subsystem of the Reverse Saturation Current on Simulink

Shunt resistance current, I_{sh}, is the electric current that is allowed to pass around another point in a circuit through a low resistance path.

$$I_{sh} = [(V_t + (I * R_s)/R_{sh}] \quad 11$$

Where V_t is the diode thermal voltage, R_{sh} is the shunt resistance and R_s is the series resistance. Fig. 3.10 is the representation of the equation in Eqn. 11 using Simulink blocks. These blocks are interconnected to produce the output which is then used to form a subsystem.

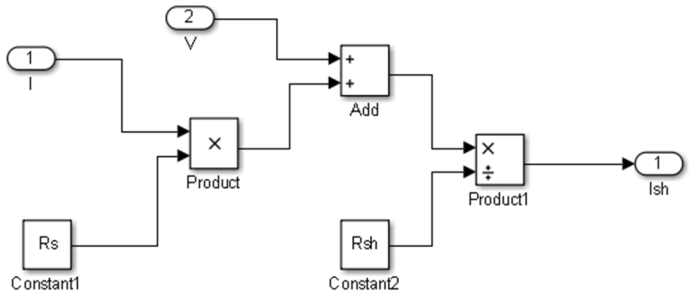


Fig 2.9: A model of Shunt current equation on Simulink

Fig. 2.10 is the subsystem of the equation in Fig. 2.9 which is combined to form a single system of an output and input.

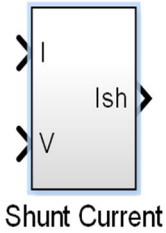


Fig 2.10: A subsystem of the Shunt Current on Simulink

Output Current, I, which is also known as the rated output current is the maximum load current that a power supply can provide at a specified ambient temperature. A power supply can never provide more current than its rated output unless there is a fault, such as short circuit at the load. The output current can be calculated as shown in Eq. 12.

$$I = I_{ph} - I0\left[\exp\left(q\left[V_t + \frac{I*R_S}{n} * K * N_s * T\right]\right) - I_{sh}\right] \quad 12$$

Fig. 3.12 is the subsystem of the equation in Fig. 3.12 which is combined to form a single system of an output and input.

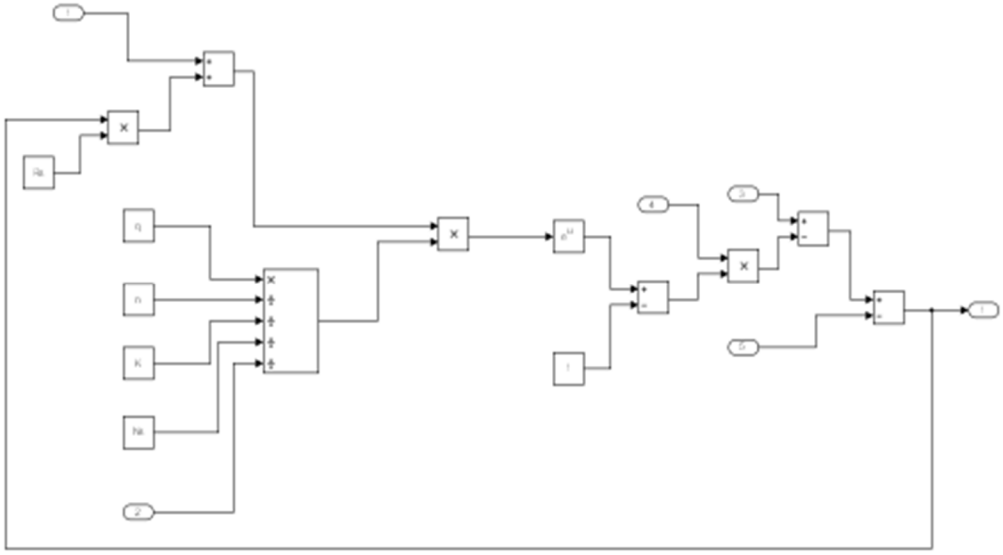


Fig 2.11: A model of PV Output current equation on Simulink

Fig. 2.12 is the subsystem of Fig. 2.11 which is combined to form a single system of an output and input.

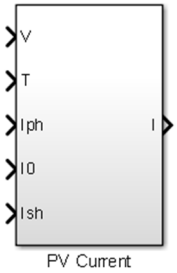


Fig 2.12: A subsystem of the PV Output current on Simulink

Subsequently the various subsystems that were modelled into a single system to make up the off-grid photovoltaic panel depicting the core parameter of the system that includes the Operating Temperature, T, the output Current, I, the output Voltage , V , and the Solar irradiance, G. Each subsystem is made up of mathematical equations which typifies the electrical characteristics of a photovoltaic module.

Fig. 3.14 is the complete interconnection of all the systems from all the several subsystems. This is the off-grid photovoltaic system.

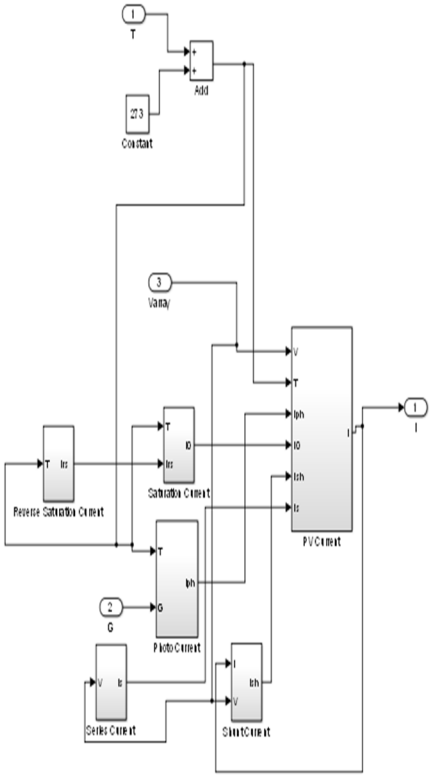


Fig 2.13: A complete assembly of all the subsystems that make up the off-grid Photovoltaic system.

Fig. 2.14 is the subsystem of Fig. 2.13 which is combined to form a single system of an output and input.

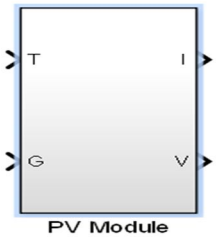


Fig 2.14: A subsystem of the photovoltaic module.

ISSN: 2321-9653; IC Value: 45.98; SJ Impact Factor: 7.538
Volume 14 Issue III Mar 2026- Available at www.ijraset.com

Fig 3.16 is the total subsystems that is combined to form the off-grid photovoltaic panel. This is connected to a P-V and I-V scope to display of the simulated results in two different scopes. The first is to show the output current, I, in relation to the Voltage, V. This displays the variation of the output current with the output voltage on a scope. The second scope displays the output power of the photovoltaic system, P, in relation to the output voltage, V.

In this model, it is assumed that the system is operating under Standard Testing Conditions with a solar irradiance of 1000W/m^2 and an operating temperature of 25^{0}C (which is equal to 273K).

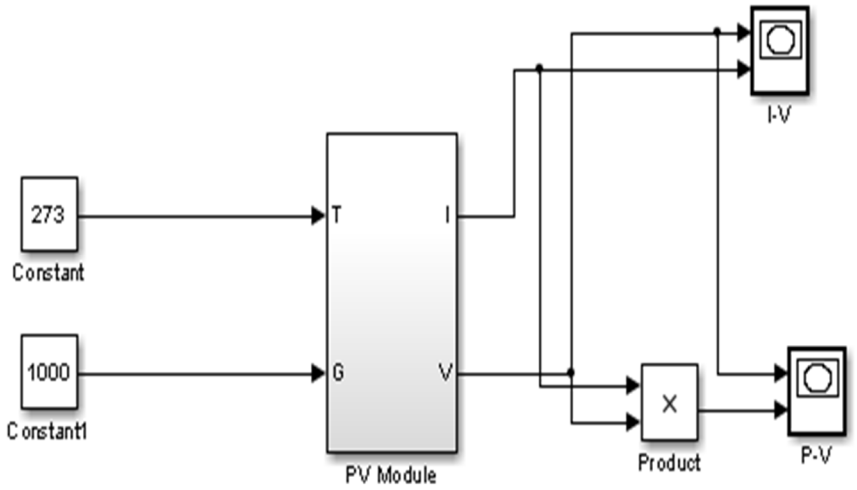


Fig 2.15: An off-grid Photovoltaic System connected to the P-V and I-V scope.

IV. RESULTS AND DISCUSSION

In this research work, the photovoltaic system was operated under a Standard Testing Condition of a solar irradiance 1000 W/m^2, 25^{0}C. The system was observed at intervals over a 72-hour period. Simulation results are shown as follows table 3.0.

Table 3.0: Results obtained from the variation of the Area of the PV system and the output Current, Voltage and Power.

AREA (m^2)	CURRENT,I (Amp)	VOLTAGE,V (Volts)	POWER,P (Watts)
1.65	9.226	36.9	340.4
1.66	9.226	36.9	340.4
1.67	9.226	36.9	340.4
1.68	9.226	36.9	340.4
1.69	9.225	36.9	340.4
1.70	**9.226**	**36.9**	**340.4**
1.71	9.226	36.9	340.4
1.72	9.226	36.9	340.4
1.73	9.226	36.9	340.4
1.74	9.226	36.9	340.4
1.75	9.226	36.9	340.4

The results from the table shows that there is no marked change in the values of the output current, output voltage and maximum power of the PV system when the Area is varied. There was a slight variation of 0.001A when the area was varied from 1.69 to 1.70. Further increase and decrease of the area did not however result in any change in the output current, voltage and power as shown in Fig. 4.1. This implies that the area of the PV panel is independent of the output current, voltage and power.

©IJRASET: All Rights are Reserved | SJ Impact Factor 7.538 | ISRA Journal Impact Factor 7.894 |

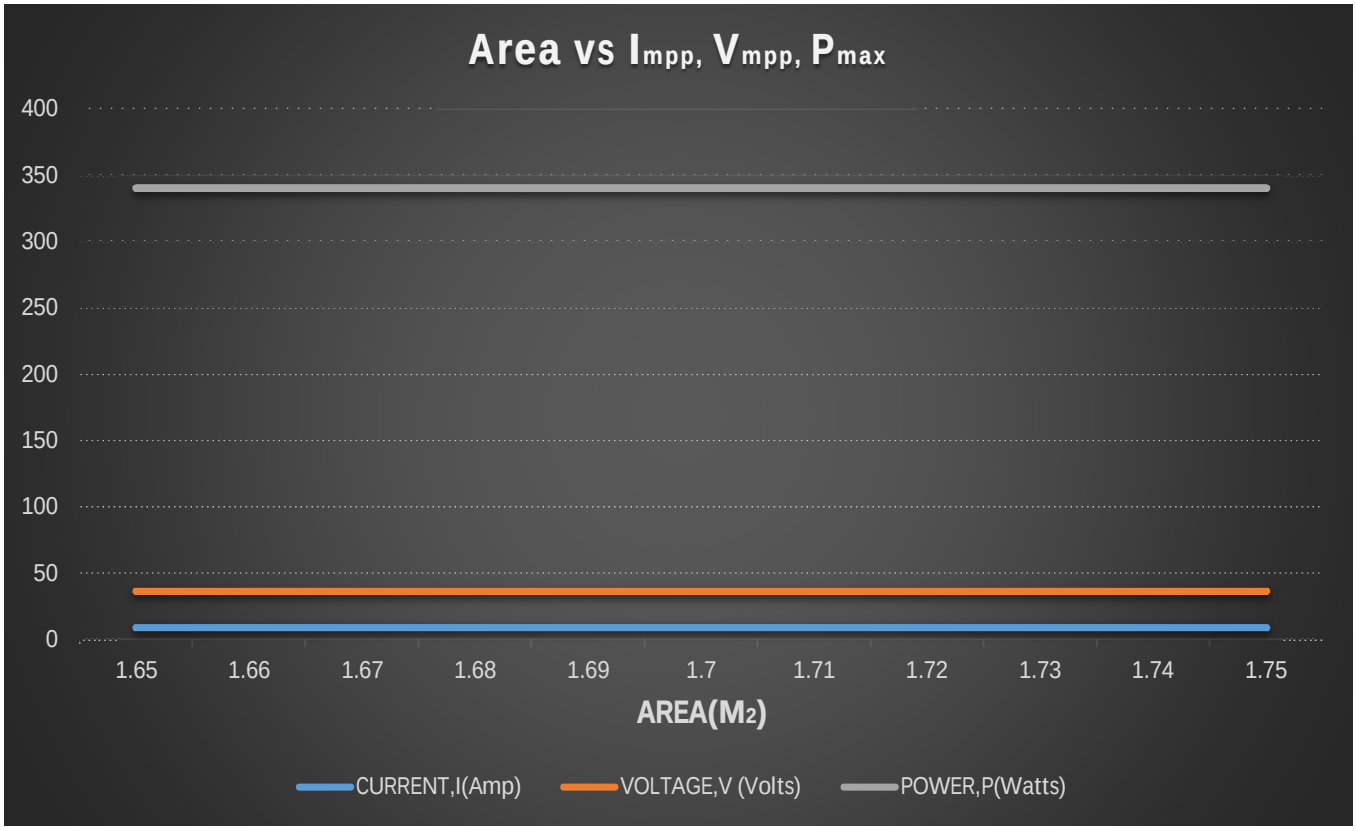


Fig 3.1: A graphical representation of the PV Area vs I_{mpp}, V_{mpp} and $P_{max.}$

The fig 4.2 shows the graphical plot of area versus the maximum power point Current (I_{mpp}), maximum power point Voltage (V_{mpp}) and the maximum Power (P_{max}) in single line and bar chart formats respectively.

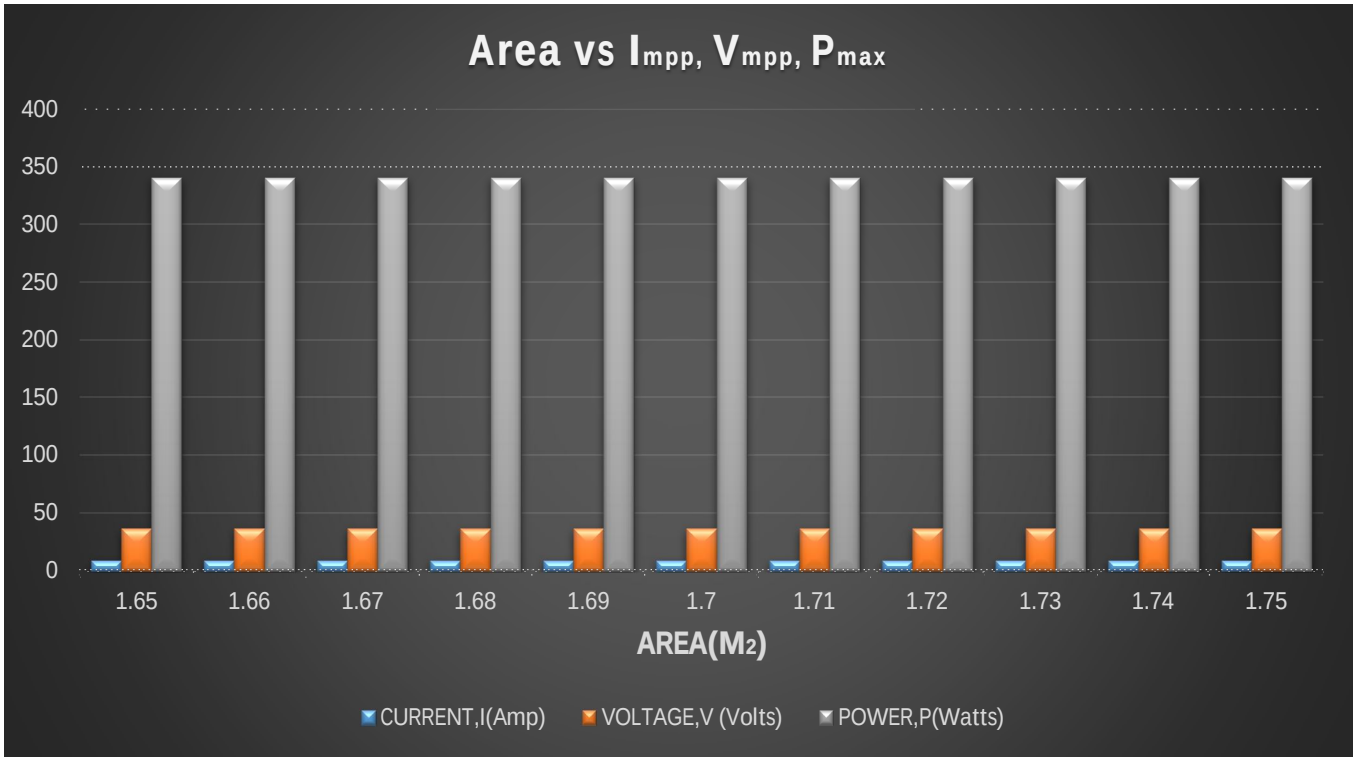


Fig 3.2: A Bar Chart representation of the PV Area vs I_{mpp}, V_{mpp} and $P_{max..}$

It can be observed that the change in the area of the photovoltaic only causes a slight decrease of 0.001A that was caused as a result of the variation of the area of the photovoltaic panel with respect to the input current. This has clearly shown that the area or size of the photovoltaic module is independent of the output current, Voltage and Power of the system. In other words, a large increase or decrease in the area/dimensions of the photovoltaic module does not lead to any significant change in the output parameters.

The Fig. 4.3 and 4.4 show the graphical representations of the output current and output Voltage with respect to the output voltage respectively.

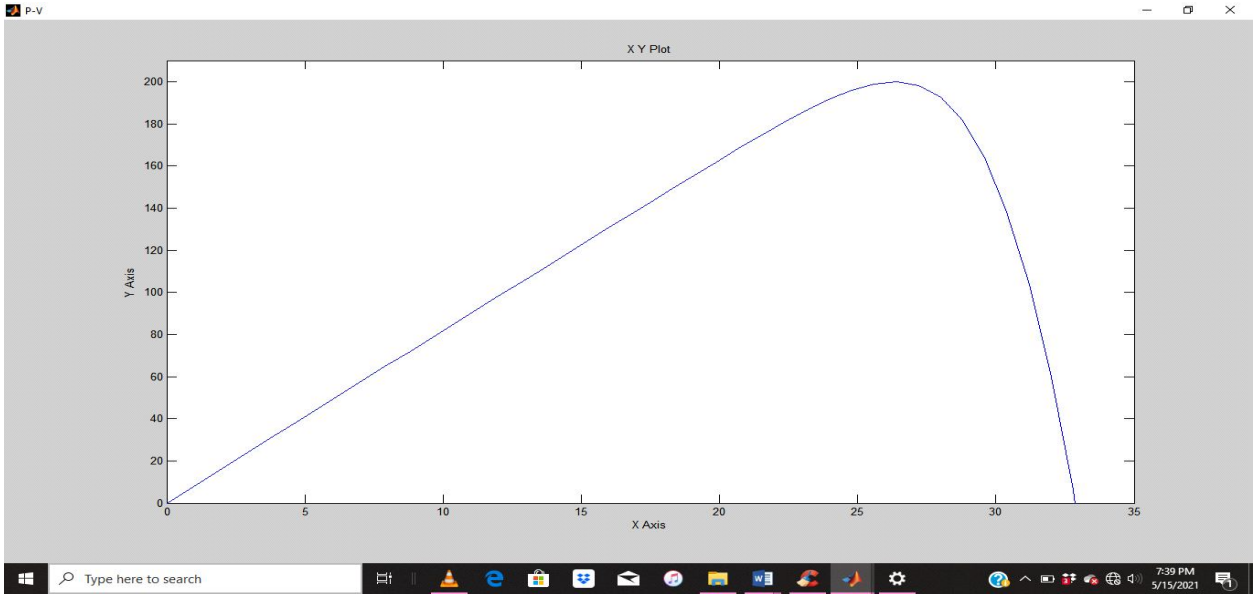


Fig 3.3: A graphical representation of the P-V curve showing Maximum Power Point Tracking

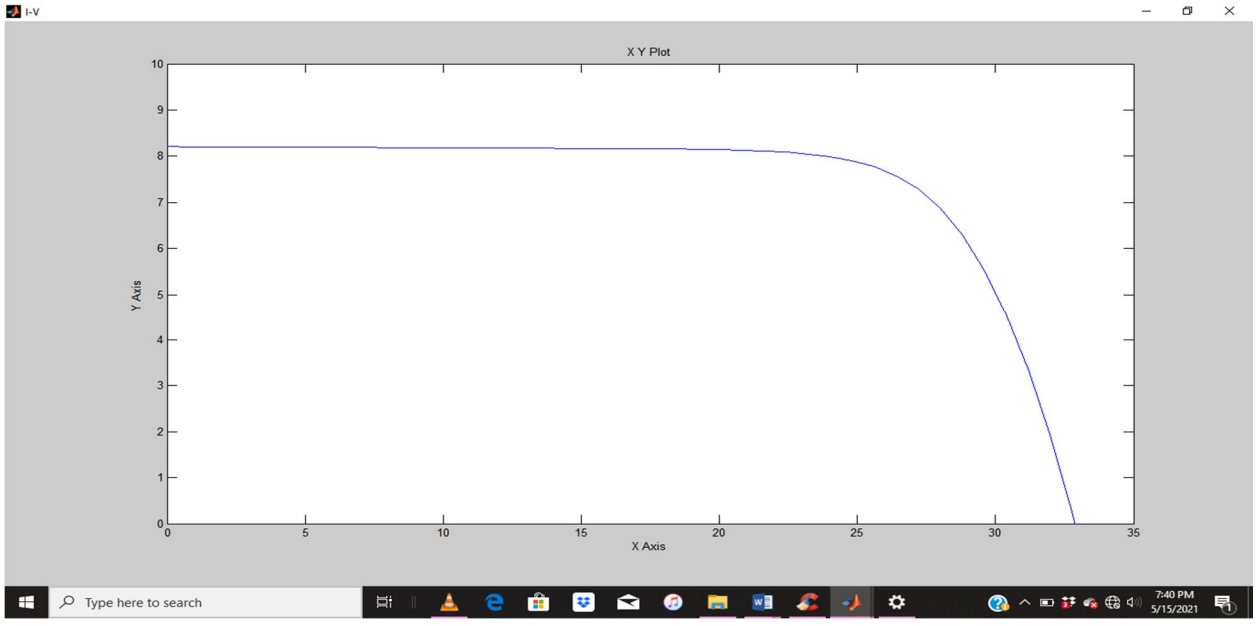


Fig 3.4: A graphical representation of the I-V curve

This show the variation of the output power of the simulation model of the photovoltaic subsystem in relation to the Output Voltage. The Y-axis represents the output power as it rises from 0w to 400w while the X-axis represents the output voltage as it increases from 0V to 40V.

The maximum power of the photovoltaic system can be seen at the tip of the curve where the current and the voltage is at its maximum. This point is known, as the Maximum Power Point Tracking (MPPT) of the photovoltaic system.it is the point at which the photovoltaic system produces its maximum power to supply to the load.

©IJRASET: All Rights are Reserved | SJ Impact Factor 7.538 | ISRA Journal Impact Factor 7.894 |

As the load demand is varied, the photovoltaic module supplies the power required to satisfy the load demand. The excess energy is supplied to the battery, which is connected to a bidirectional DC/DC converter for controlling the voltage and the current, then connected to an inverter and then to an AC load.

When the photovoltaic module is unable to supply enough energy to satisfy the power requirement of the load demand the system experiences an energy deficit and therefore the power shortfall is drawn from the battery and supercapacitor hybrid energy system that serves as a backup energy source for the entire off-grid system.

A. Discharging Mode Of The Battery

Using a controlled current source as displayed in Fig 4.5, which is connected to a load of 12.5A, State of charge and current remaining constant at 50% and 100Ah respectively, we obtain the following:

I_{out} = 12.5A, and SOC = 50% with V_{out} remaining constant at 13.78V

The discharge process is observed to be relatively fast.

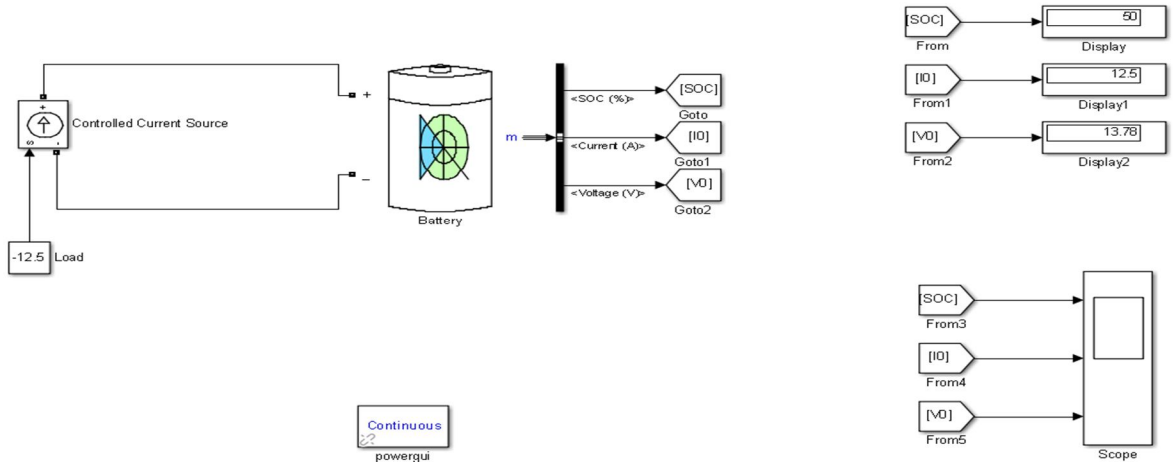


Fig 3.5 : A Lead-Acid battery connected to DC Load (Discharging mode)

The Fig. 4.6 show the graphical representations of the output current and output Voltage with respect to the output voltage of the discharging process of a lead acid battery.

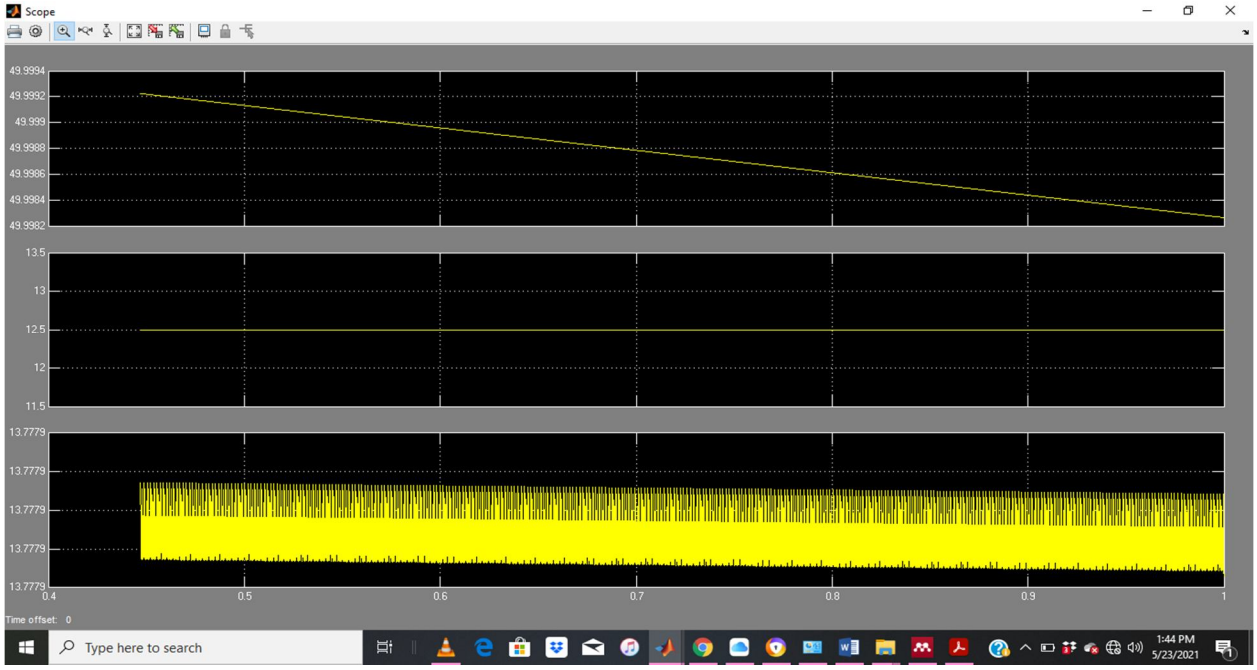


Fig 3.6: A graphical representation of the discharging process of a Lead Acid battery

B. Charging Mode Of The Battery

Using a controlled current source that is connected to a load of 10A as displayed in Fig 4.7, State Of Charge and current remaining constant at 50% and 100Ah respectively, we obtain the following:

Iout = -10A, and SOC = 50.0007% with Vout remaining constant at 13.81V

The charging sequence is observed to be relatively slow over the time period.

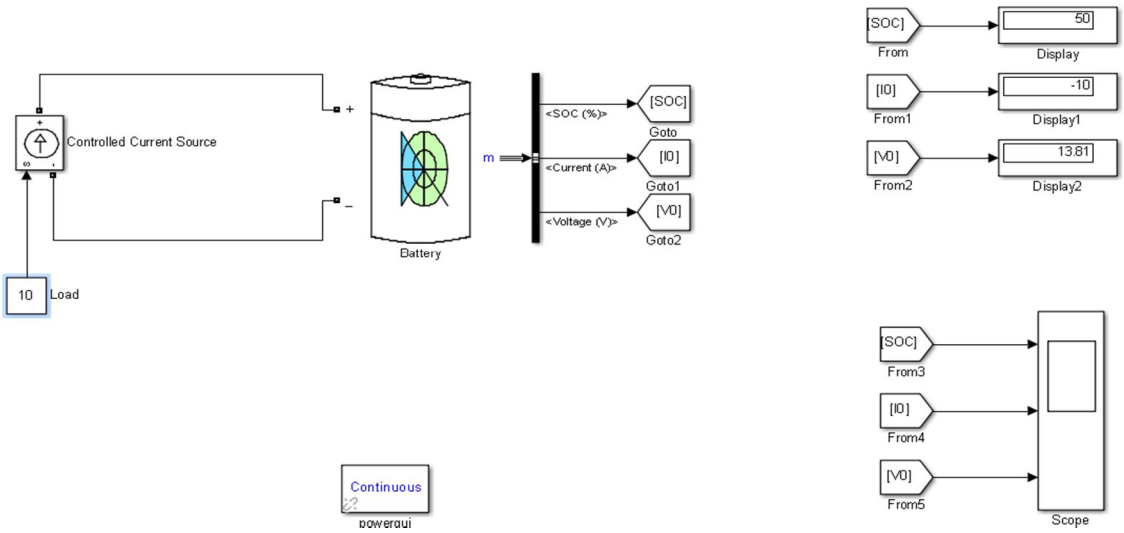


Fig 3.7 : A Lead acid battery connected to DC Load (Charging mode)

The Fig. 4.6 show the graphical representations of the output current and output Voltage with respect to the output voltage of the charging process of a lead acid battery.

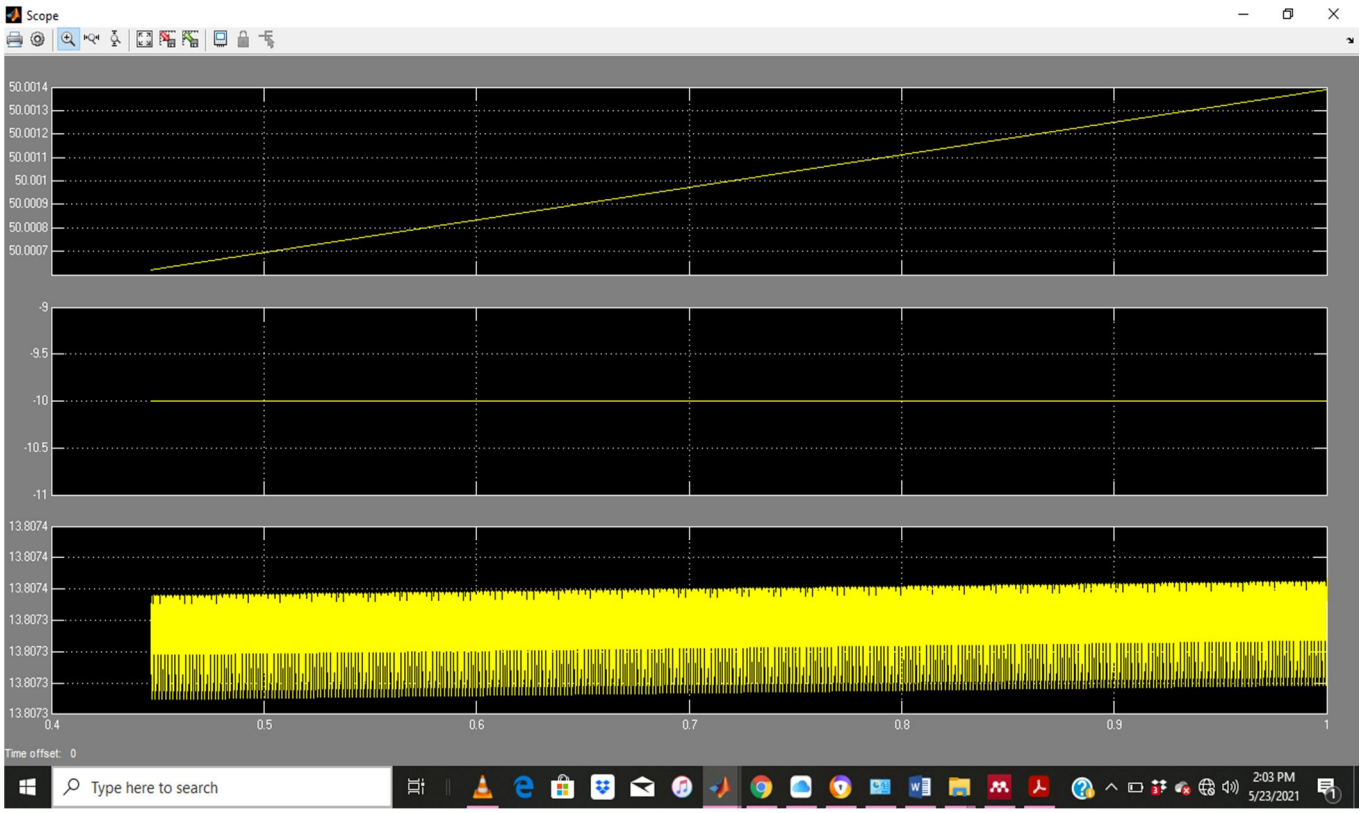


Fig 3.8: A graphical representation of the charging process of a Lead acid battery.

V. CONCLUSIONS

In this work, the output current decreased by 0.001A but an increase in the area did not result in any significant change on the output current and voltage. This shows that the area of the photovoltaic panel is independent of the output current , voltage and power. It was also observed that the supercapacitor helps in boosting the charging capacity of the battery and reduces its discharge. The supercapacitor possesses unique properties that can complement other energy storage technologies, such as batteries due to its fast charge and discharge capability, highly reversible process functionality, high power density, high recyclability and relatively small internal resistance.

It is an attractive alternative in hybrid electric energy systems. An equivalent supercapacitor model was formalized based on electric characterization, which was used in simulations of the off-grid PV/HESS model. When characterizing the supercapacitor, a capacitance voltage dependency was detected, which is important to take into account, since it affects the output current and voltage of the hybrid energy system. When conducting simulations of the passive hybrid system, it was found that the model probably should be simplified in order to adequately capture the system's short-term behavior under transient loading.

Regarding performance of the system, we found that when the resistance of the applied load demand was varied, the passive hybrid system could in theory meet a pulse load amplitude up to nine times as large as the rated power of the battery. The simulation confirmed that the power rating of the system can be increased by hybridization,

The output current decreased with decreasing area of the panel while it remained fairly constant with increasing area of the photovoltaic panel.

It was found that when the system experiences increase in load demand the state of charge of the battery-only system experienced a sharp decline or slow charge with respect to the amount of current that is being supplied from the photovoltaic panel. On the other hand, when load demand is being varied using the battery-supercapacitor hybrid system the battery experienced a slow discharging and fast charging. This is as a result of the supercapacitor being utilized, relieving the battery of large voltage fluctuations and reducing the maximum battery current.

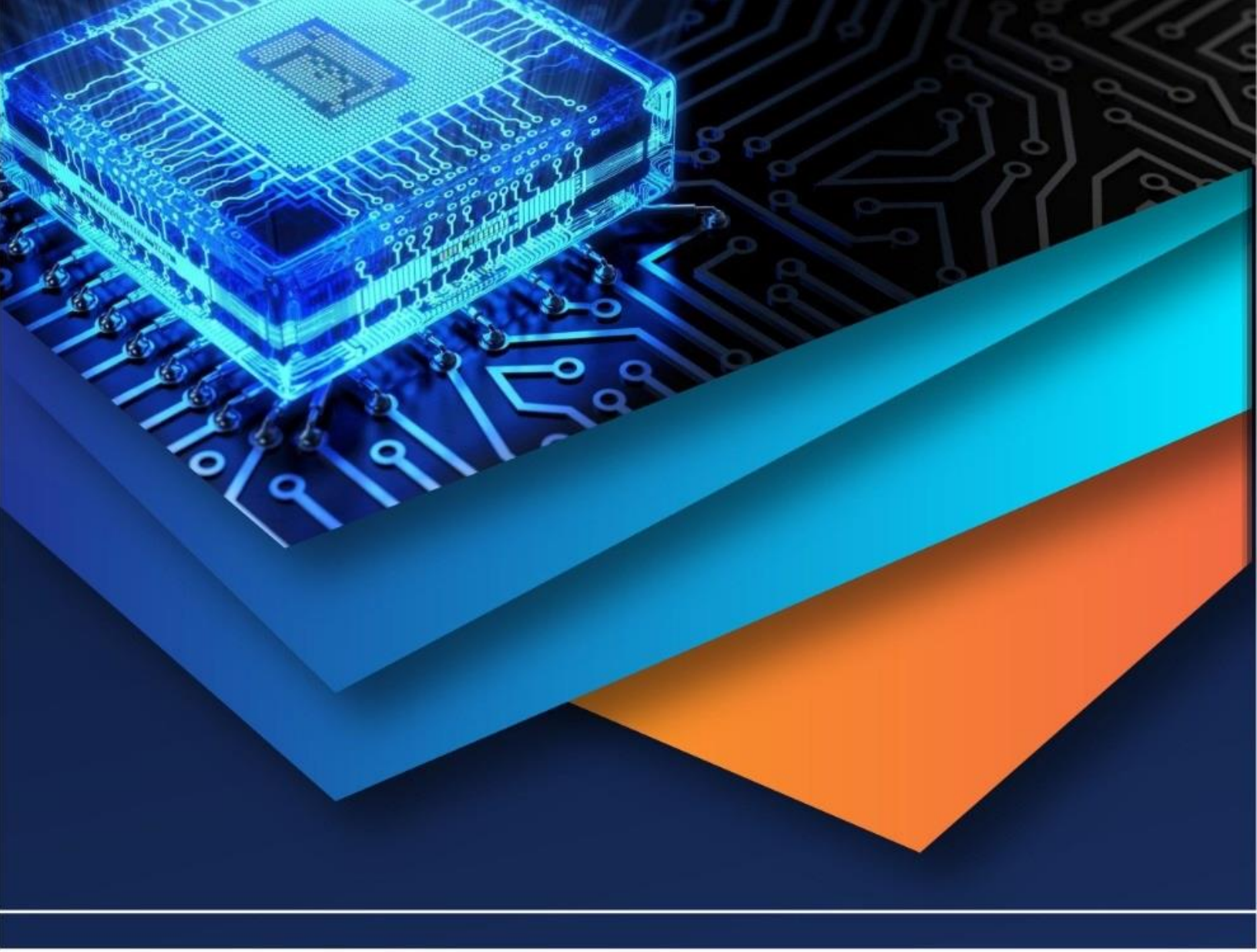
REFERENCES

[1] Al-salaymeh, A., Al-hamamre, Z., Sharaf, F. & Abdelkader, M.R. 2010. Technical and economical assessment of the utilization of photovoltaic systems in residential buildings : the case of jordan. Energy Conversion and Management 51(8): 1719–1726.
[2] M.S. Whittingham, "History, Evolution, and Future Status of Energy Storage," Proc. IEEE, vol. 100, pp. 1518-1534, May 2012, DOI: 10.1109/jproc.2012.2190170
[3] "RCUK Energy Programme: What the Energy Programme funds." Research Councils UK, Polaris House, North Star Ave, Swindon, SN2 1ET, [Online], Access date: Jul. 2012, Available: http://www.rcuk.ac.uk/research/xrcprogrammes/energy/EnergyResearch/Pages/SUPERGEN.asx
[4] M. Venables, "Closing in on 2020," Engineering & Technology, vol. 7, pp. 28-31, Feb. 2012
[5] B. De Wachter. "Connecting Distributed Generation (DG) units to the network." Leonardo Energy, London, Jul., 2008., [Online], Access date: Jul. 2012, Available: http://www.leonardo-energy.org/connecting-distributed-generation-dg-units-network
[6] M.R. Student, R. Hidalgo, C. Abbey, and G. Joos, "An Expert System for optimal scheduling of a diesel - wind - energy storage isolated power system," Industrial Electronics, 2009. IECON '09. 35th Annual Conference of IEEE, Porto, Portugal, 2009, pp. 4293-4298.
[7] G. Coppez, S. Chowdhury, and S.P. Chowdhury, "The importance of energy storage in Renewable Power Generation: A review," Universities Power Engineering Conference (UPEC), 2010 45th International, Cardiff, Wales, 2010, pp. 1-5.
[8] G. Coppez, S. Chowdhury, and S.P. Chowdhury, "South African renewable energy hybrid power system storage needs, challenges and opportunities," Power and Energy Society General Meeting, 2011 IEEE, Detroit, MI, 2011, pp. 1-9.
[9] H. Bindner, T. Cronin, P. Lundsager, J.F. Manwell, U. Abdulwahid, and I. Baring-Gould, "Lifetime modelling of lead acid batteries," Risø Nat. Lab., Roskilde, Denmark, Apr. 2005.
[10] N. Garimella and N.K.C. Nair, "Assessment of battery energy storage systems for small-scale renewable energy integration," TENCON 2009 - 2009 IEEE Region 10 Conference, Singapore, 2009, pp. 1-6.
[11] V. Svoboda, Wenzl, H., Kaiser, R., Jossen, A., Baring-Gould, I., Manwell, J., Lundsager, P., Bindner, H., Cronin, T., Nørgård, P., Ruddell, A., Perujo, A., Douglas, K., Rodrigues, C., Joyce, A., Tselepis, S., van der Borg, N., Nieuwenhout, F., Wilmot, N., Mattera, F., and D. Sauer, "Operating conditions of batteries in off-grid renewable energy systems," Solar Energy, vol. 81, pp. 1409-1425, 2007
[12] N. Kularatna, "Rechargeable batteries and their management," IEEE Instrum. Meas. Mag., vol. 14, pp. 20-33, April 2011, DOI: 10.1109/mim.2011.5735252
[13] L. Peiwen, "Energy storage is the core of renewable technologies," Nanotechnol. Mag., vol. 2, pp. 13-18, Dec. 2008, DOI: 10.1109/MNANO.2009.932032
[14] A. Etxeberria, I. Vechiu, H. Camblong, and J.M. Vinassa, "Hybrid Energy Storage Systems for renewable Energy Sources Integration in microgrids: A review," International Power and Energy Conference, IPEC, 2010 Conference Proceedings, Singapore, 2010, pp. 532-537. 214
[15] B.R. Alamri and A.R. Alamri, "Technical review of energy storage technologies when integrated with intermittent renewable energy," Sustainable Power Generation and Supply, 2009. SUPERGEN '09. International Conference on, Nanjing, China, 2009, pp. 1-5.
[16] P.J. Hall and E.J. Bain, "Energy-storage technologies and electricity generation," Energy Policy, vol. 36, pp. 4352-4355, Oct. 2008, DOI: 10.1016/j.enpol.2008.09.037
[17] G. Plante, The Storage of Electrical Energy. Whitefish, MT Publisher Kessinger Publishing, 2007 1859 ISBN: 9781154857726

©IJRASET: All Rights are Reserved | SJ Impact Factor 7.538 | ISRA Journal Impact Factor 7.894 |

[18] R. Sebastian and R. Pena-Alzola, "Study and simulation of a battery based energy storage system for wind diesel hybrid systems," Energy Conference and Exhibition (ENERGYCON), 2012 IEEE International, Florence, Italy 2012, pp. 563-568.
[19] D. Gielen, "Electricity Storage and Renewables for Island Power: A Guide for Decision Makers," ed: IRENA (International Renewable Energy Agency), 2012.
[20] T. Lambert, P. Gilman, and P. Lilienthal, "Micropower system modeling with HOMER," Integration of Alternative Sources of Energy ed New York: John Wiley & Sons, 2006.
[21] G. Coppez, S. Chowdhury, and S.P. Chowdhury, "Review of battery storage optimisation in Distributed Generation," Power Electronics, Drives and Energy Systems (PEDES) & 2010 Power India, 2010 Joint International Conference on, New Delhi, India, 2010, pp. 1-6.
[22] V. Musolino, L. Piegari, and E. Tironi, "New full frequency range supercapacitor model with easy identification procedure," IEEE Trans. Ind. Electron., vol. PP, pp. 1-1, Aug. 2012, DOI: 10.1109/tie.2012.2187412
[23] H.I. Becker, "Low voltage electrolytic capacitor " United States Patent US patent 2800616, 23 July 1957.
[24] J. Schindall, "The Charge of the Ultracapacitors," IEEE Spectr., vol. 44, pp. 42-46, 2007, DOI: 10.1109/mspec.2007.4378458
[25] B.E. Conway, Electrochemical supercapacitors : scientific fundamentals and technological applications. New York: Plenum Press, 1999. ISBN: 9780306457364
[26] G.L. Bullard, H.B. Sierra-Alcazar, H.L. Lee, and J.L. Morris, "Operating principles of the ultracapacitor," IEEE Trans. Magn, vol. 25, pp. 102-106, Jan. 1989, DOI: 10.1109/20.22515
[27] A.F. Burke, J.E. Hardin, and E.J. Dowgiallo, "Application of ultracapacitors in electric vehicle propulsion systems," Power Sources Symposium, 1990., Proceedings of the 34th International, Cherry Hill, NJ, 1990, pp. 328-333.
[28] Z. Haihua, T. Bhattacharya, T. Duong, T.S.T. Siew, and A.M. Khambadkone, "Composite Energy Storage System Involving Battery and Ultracapacitor With Dynamic Energy Management in Microgrid Applications," IEEE Trans. Power Electron., vol. 26, pp. 923-930, Mar. 2011, DOI: 10.1109/IPEC.2010.5543543
[29] S. Vazquez, S.M. Lukic, E. Galvan, L.G. Franquelo, and J.M. Carrasco, "Energy Storage Systems for Transport and Grid Applications," IEEE Trans. Ind. Electron., vol. 57, pp. 3881-3895, Dec. 2010, DOI: 10.1109/tie.2010.2076414
[30] H. Tai-Sik, M.J. Tarca, and P. Sung-Yeul, "Dynamic Response Analysis of DC-DC Converter With Supercapacitor for Direct Borohydride Fuel Cell Power Conditioning System," IEEE Trans. Power Electron., vol. 27, pp. 3605-3615, 2012, DOI: 10.1109/tpel.2012.2185711 215
[31] P.H. Mellor, N. Schofield, and D. Howe, "Flywheel and supercapacitor peak power buffer technologies," Electric, Hybrid and Fuel Cell Vehicles (Ref. No. 2000/050), IEE Seminar, 2000, pp. 8/1-8/5.
[32] S. Lemofouet and A. Rufer, "A Hybrid Energy Storage System Based on Compressed Air and Supercapacitors With Maximum Efficiency Point Tracking (MEPT)," IEEE Trans. Ind. Electron., vol. 53, pp. 1105-1115, 2006, DOI: 10.1109/tie.2006.878323

©IJRASET: All Rights are Reserved | SJ Impact Factor 7.538 | ISRA Journal Impact Factor 7.894 |



10.22214/IJRASET

45.98

IMPACT FACTOR: 7.129

IMPACT FACTOR: 7.429

INTERNATIONAL JOURNAL FOR RESEARCH

IN APPLIED SCIENCE & ENGINEERING TECHNOLOGY

Call : 08813907089 (24*7 Support on Whatsapp)